10th International Conference on Fracture Mechanics of Concrete and Concrete Structures
FraMCoS-X
G. Pijaudier-Cabot, P. Grassl and C. La Borderie (Eds)
https://doi.org/10.21012/FC10.235471

# ON THE SYNERGETIC ACTION BETWEEN STRAIN-HARDENING CEMENT-BASED COMPOSITES (SHCC) AND CARBON TEXTILE REINFORCEMENT UNDER TENSILE LOADING

**TING GONG[†*], AHMED AMEER HAMZA[†], IURIE CUROSU[†] AND VIKTOR MECHTCHERINE[†]**

[†]Technische Universität Dresden (TUD)
Institute of Construction Materials, 01069, Germany
[*] e-mail: ting.gong@tu-dresden.de

**Key words:** Carbon textile reinforcement, SHCC, Bond, Tension

**Abstract:** The work at hand describes the influence of the bond properties between carbon textile reinforcement and strain-hardening cement-based composites (SHCC) on the composite tensile behavior. The SHCC matrix was reinforced with 6-mm long micro-fibers made of ultra-high molecular weight polyethylene (UHMWPE) in a volume ratio of 2 %. For emphasizing the benefits of hybrid fiber reinforcement, the cementitious matrix with 0 % short fibers was reinforced with carbon textile only. Specially designed specimens were tested in tension under a displacement rate of 0.05 mm/s. The deformation, crack formation and fracture of the tested specimens were monitored optically and subsequently evaluated using Digital Image Correlation (DIC).

## 1 INTRODUCTION

Strain-hardening cement-based composites (SHCC) [1] and textile reinforced concrete (TRC) [2,3] are two types of novel fiber reinforced composites which yield a ductile behavior under increasing tensile loading. SHCC consist of finely grained cementitious matrices and short high-performance polymer fibers, while TRC is reinforced with continuous two- or three-dimensional textile layers consisting of carbon, polymer or alkali-resistant glass yarns. Both types of composites exhibit high inelastic deformations in the strain-hardening phase as a result of the successive formation of multiple fine cracks. In comparative terms SHCC show more pronounced multiple cracking and higher strain capacity, while TRC yields higher tensile strength.

For the purpose of structural strengthening against severe dynamic actions, the application of thin strengthening layers combining both reinforcing principles is highly promising. The combination of SHCC and TRC should result in composites with high tensile strength, enhanced crack control and high stiffness in cracked state. Furthermore, the spatial confinement of the matrix by short micro-fibers results in a larger energy dissipation capacity and higher damage tolerance, both features being of high importance under highly dynamic actions.

The favorable and efficient synergetic effect of a hybrid fiber reinforcement requires a purposeful material design based on a clear understanding of the mechanical interactions in the composites. These mechanisms have been investigated by the authors in the framework of the Research Training Group GRK 2250 [4,5].

The paper at hand presents some representative results of quasi-static tests with emphasis on the bond properties between the carbon textile reinforcement and the SHCC matrix. The study involved a carbon textile with two different coatings for simulating a moderate and a strong bond, respectively, while the textile reinforcement ratio was 0.75 % in both cases. The adopted matrix material was a high-strength SHCC, which was extensively investigated by the authors under various loading conditions in previous studies [6,7]. Additionally, for highlighting the advantages of hybrid fiber-reinforcement, the constitutive matrix of SHCC was strengthened with the carbon textile only, i.e. no short fiber was used. Finally, for evaluating the deformation capacity of the textile yarns, the textile reinforcement was tested separately on samples with representative dimensions.

The specimens were tested in uniaxial tension in a hydraulic testing machine with a controlled displacement rate of 0.05 mm/s. The deformations and fracture processes were monitored optically and subsequently evaluated using Digital Image Correlation (DIC).

## 2 MATERIALS

### 2.1 Matrix

The high-strength finely grained matrix was specifically designed for high-strength SHCC reinforced with short high-performance polymer fibers Dyneema®, produced by DSM, the Netherlands [7].

**Table 1**: Mixture composition of the high-strength cementitious matrix

| Components | $kg/m^3$ |
|---|---|
| CEM I 52.5R-SR3/NA | 1460 |
| Silica fume | 292 |
| Quartz sand 0.06-0.2 mm | 145 |
| Superplasticizer, PCE | 45 |
| Water | 315 |

The matrix has a high cement content in combination with silica fume as additional binder. The water-to-binder ratio is 0.18; see Table 1. Only a small amount of fine sand was used, since the nature and geometry of the polymer micro-fibers as well as the need of their uniform distribution over the matrix impose limitations regarding the content and size of the aggregates.

The short polymer fibers made of ultra-high molecular weight polyethylene (UHMWPE) had a length of 6 mm and a diameter of approximately 20 µm, see Table 2. The relatively small length of the fibers was chosen based on workability considerations as well as with regard to the geometry of the textile mesh, as presented in the next section.

**Table 2**: Properties of UHMWPE fibers as provided by manufacturer [8]

| | |
|---|---|
| Manufacturer | DSM |
| Brand | Dyneema® |
| Diameter | 20 µm |
| Length | 6 mm |
| Density | 970 $kg/m^3$ |
| Tensile strength | 2500 MPa |
| Modulus of elasticity | 80 GPa |
| Elongation at break | 3.5 % |

### 2.2 Carbon textile reinforcement

The investigated carbon textile was produced by V.FRAAS GmbH under the designation of SITgrid 040, see Figure 1. The spacings between the warp (reinforcing) yarns and weft (transversal) yarns are 12.7 mm and 16 mm, respectively.

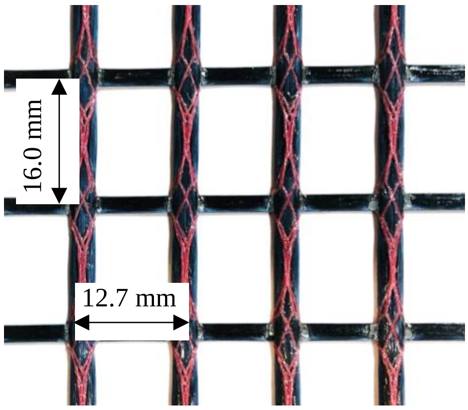


**Figure 1**: Textile reinforcement under investigation.

The average yarn count for warp direction is 3200 tex and 800 tex for the weft direction. The acrylate coating was applied directly during the production process. The textile in this form is named T1 in the article at hand; see also

Figure 2a. The acrylate coating yields a moderate bond strength with the surrounding cementitious matrix. For ensuring a considerably stronger bond, the same textile was additionally coated manually with epoxy resin and sand; see Figure 2b. The extra-coated textile carries the denomination T2.

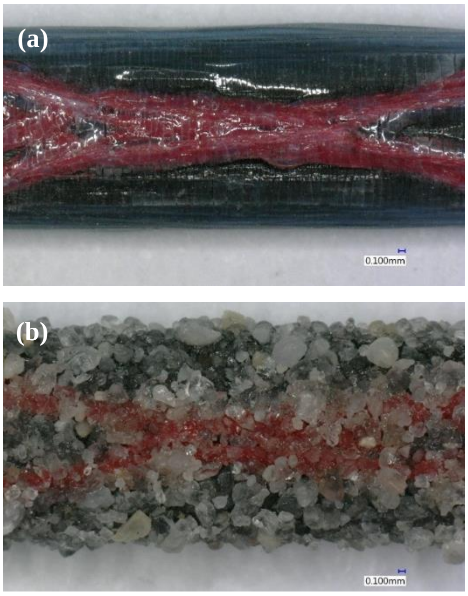


**Figure 2**: Carbon yarns with different coatings: (a) T1 with acrylate coating and (b) T2 with extra coating of epoxy resin and sand.

## 3 TESTING CONFIGURATION

### 3.1 Specimens

The uniaxial tension tests on cement-based composites were conducted using plate-like specimens with a tapered gauge portion. The specimens had a constant thickness of 20 mm and a total length of 700 mm. The 275 mm long and 100 mm wide end portions served as textile anchorage zones as well as for the mechanical gripping during the tension tests. Textile T1 was also coated with epoxy and sand at both ends, i.e. in the clamping zones, in order to exclude any yarn pullout after matrix cracking.

The gauge portion in the middle of the specimens had a length of 150 mm and a width of 60 mm; see Figure 3a.

All specimens were reinforced with only one layer of textile, which means an effective reinforcement ratio of 0.75 %, calculated based on the effective cross-sectional area of 1.8 mm$^2$ of each warp yarn. Five warp yarns strengthened the specimens in the loading direction.

The specimens consisting of SHCC matrix and textile were produced by using a lamination technique. The first layer of SHCC was cast in the molds prior to the placement of textile reinforcement. Subsequently, the textile mesh was gently pressed into the SHCC matrix so that the latter could penetrate through the textile mesh. At the same time, care was taken to place the carbon meshes in the middle of the specimen thickness. The second layer of the matrix was then cast on top followed by leveling and smoothening. The specimens were demolded at an age of 24 hours, sealed in plastic sheets and subsequently cured for 27 days in a climatic chamber with constant temperature of 20 °C and relative humidity of 65 %.

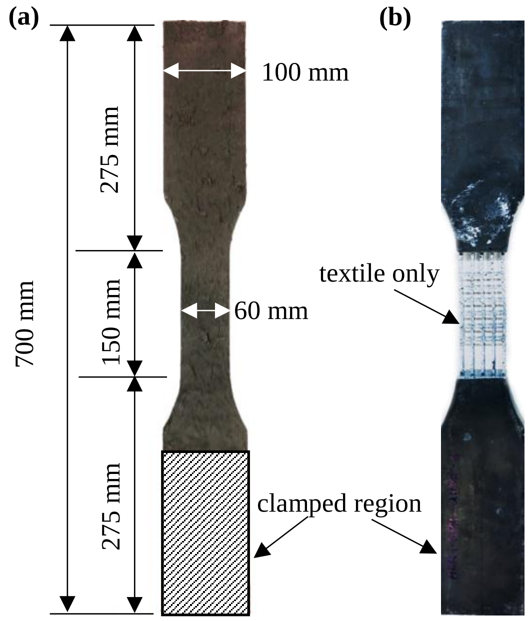


**Figure 3**: Geometry and dimensions of the (a) composite specimens and (b) specimens for testing textile.

The tension tests on the textile meshes were performed using the same molds, but without filling the gauge zone with matrix material, see Figure 3b.

In the current paper the combination between SHCC and standard (acrylate) textile will be named T1-SHCC, and with extra-coated textile T2-SHCC. The corresponding combinations of non-reinforced cementitious matrix and textile will be named T1-M and T2-M, respectively.

### 3.2 Testing setup

Special clamping devices were designed and produced to ensure a rigid physical connection between the tested specimens and the machine as shown in Figure 4. The transversal clamping pressure was generated at both specimen's ends by hydraulic jacks. The clamping plates had a roughened inner surface for a better grip. A pressure of 10 MPa was applied to ensure a secure fixation of the specimens within the clamps and to avoid slippage.

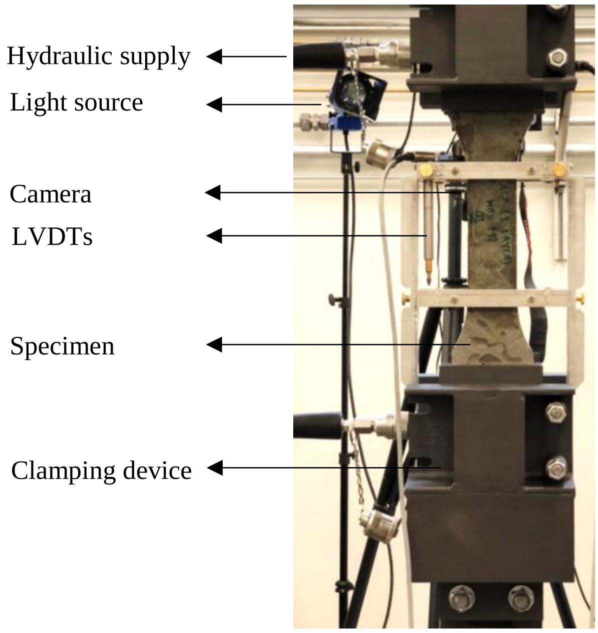


**Figure 4**: Testing configuration.

The uniaxial tension tests were done in an Instron 8501 hydraulic testing machine under a controlled displacement rate of 0.05 mm/s. The deformations of the gauge portion were measured by two Linear Variable Differential Transformers (LVDTs) positioned on both sides of the specimens.

Additionally, the deformations, crack formation and fracture process were monitored optically and subsequently evaluated using the Digital Image Correlation (DIC) technique. The high-resolution images for DIC were done with a Canon E05 700D camera at an interval of 5 seconds. The total test duration ranged between 140 and 180 seconds. The DIC evaluation was performed using the Aramis software, by GOM GmbH.

The textile specimens (i.e. specimens without matrix) were tested in a similar way. The LVDT frame was fixed to the anchorage blocks. Additionally, optical markers were glued at both ends of the individual yarns in order to capture their elongation, while excluding the delamination occurring at their exit points from the anchorage blocks.

## 4 RESULTS AND DISCUSSION

### 4.1 Properties of textiles and SHCC matrix

Figure 5 shows the tensile behavior of the SHCC specimens without textile reinforcement. The average tensile strength of the analyzed SHCC is 6.7 MPa and the average strain at peak stress is 1.0 %. The specimens exhibit a ductile softening due to the well-balanced interaction between the cementitious matrix and the short micro-fibers, which ensures a proper utilization of the fibers' tensile strength without leading to pronounced fiber rupture.

Note that the results obtained for the SHCC specimens show a considerable scatter in terms of tensile strength and strain capacity. The issue regarding the robustness of the mechanical behavior becomes more pronounced with the size of the tested elements. The same material tested previously on smaller dumbbell-shaped specimens yielded an average tensile strain capacity of 3.9 % [7]. This is an additional indication on the necessity for a continuous reinforcement at the structural scale, which would allow better stress distribution and hinder premature crack localization.

The tensile behaviors of the textiles T1 and T2 are given in Figure 6. The collective longitudinal stress of the textile meshes was calculated according to the effective cross-sectional area of the yarns, i.e. 1.8 mm$^2$ x 5. The average tensile strength of T1 and T2 was 2911.0 MPa and 2763.3 MPa, respectively. The ultimate strain capacity as measured with LVDTs was approximately 1.6 % for both textiles.

Note that the LVDTs do not capture the elongation of the individual textile yarns and that these measurements include also the elongations at the boundaries of the yarns, i.e. at the embedment in the anchorage blocks.

The DIC evaluation according to the markers glued to the yarns yield lower deformations. Nevertheless, these results show that for the given specimen geometry the high-strength SHCC is compatible with the carbon textile in terms of deformation capacity, which is an important prerequisite for an efficient composite action. Table 3 summarizes the mechanical properties of the SHCC and textiles under investigation.

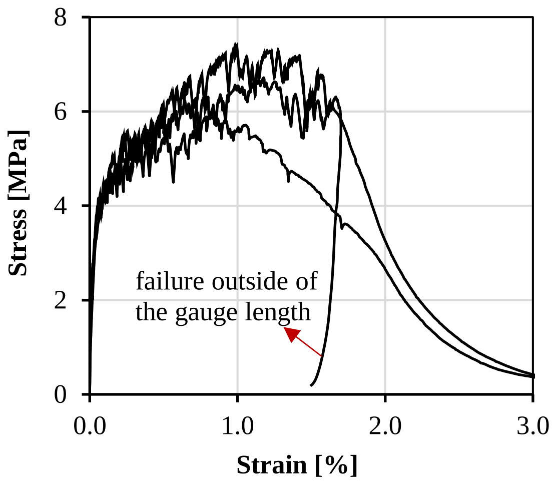


**Figure 5**: Uniaxial tensile behavior of the SHCC.

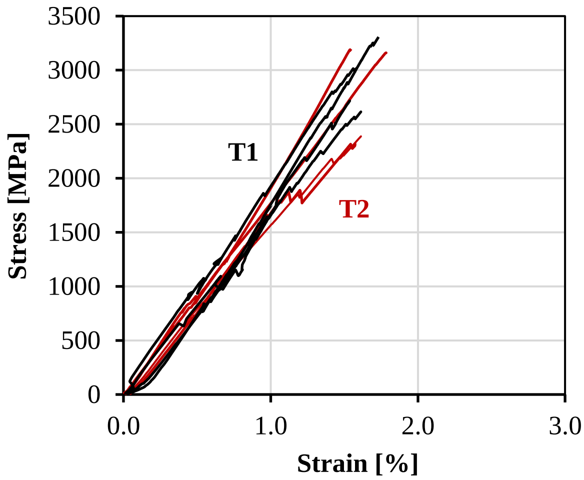


**Figure 6**: Tensile behavior of the textiles T1 and T2.

The applied coating on T2 consisting in epoxy resin and sand did not influence the mechanical behavior of the carbon yarns. The stress drops observed for the curves in Figure 6 are caused by the gradual delamination of the yarns from the cementitious anchorage blocks.

**Table 3**: Results of the uniaxial tension tests on SHCC and two different textiles as average values, standard deviations are given in parentheses

| | Matrix | Textiles | |
|---|---|---|---|
| | SHCC | T1 | T2 |
| Tensile strength (MPa) | 6.7<br>(0.7) | 2911.0<br>(308.4) | 2763.3<br>(474.8) |
| Elongation at peak (%) | 1.0<br>(0.2) | 1.6<br>(0.1) | 1.6<br>(0.1) |

## 4.2 Effect of hybrid fiber reinforcement

To show the advantages of a hybrid fiber reinforcement, the tensile stress-strain curves of four types of composites, T1-M (reference material), T1-SHCC, T2-M and T2-SHCC are presented all together in Figure 7. The plotted nominal strains were calculated based on the recordings from the LVDTs, while the stress represents the force divided by the composite cross-section of 20 mm x 60 mm. Table 4 summarizes the results of the uniaxial tension tests on the composite specimens.

The composites made of SHCC and textile reinforcement show higher stresses from the initial cracking phase up to failure, disregarding the type of textile coating, in comparison to the specimens made of textile and plain SHCC matrix. Figure 8 shows just the initial portions of the stress-strain curves up to a composite strain level of 0.4 %. The composite T1-M (without short fiber reinforcement) yields a limited extent of multiple cracking, which is followed by relatively steady hardening portions up to the failure. This pattern is characteristic for TRC [2,3,9-11]. The pronounced scattering in the initial loading stage can be traced back to shrinkage cracks as well as to the high brittleness of the plain finely grained matrix. The brittleness of the plain matrix also leads to a pronounced spalling in the composites T1-M and T2-M; see Figure 9a.

These negative effects were effectively inhibited by the short micro-fibers in T1-SHCC and T2-SHCC; see Figure 9b. The composites with hybrid fiber reinforcement show an excellent crack control in terms of crack width under increasing tensile load. Different from the typical patterns for TRC, the multiple cracking continues at larger deformations, as can be seen in Figures 7, 10b and 10d.

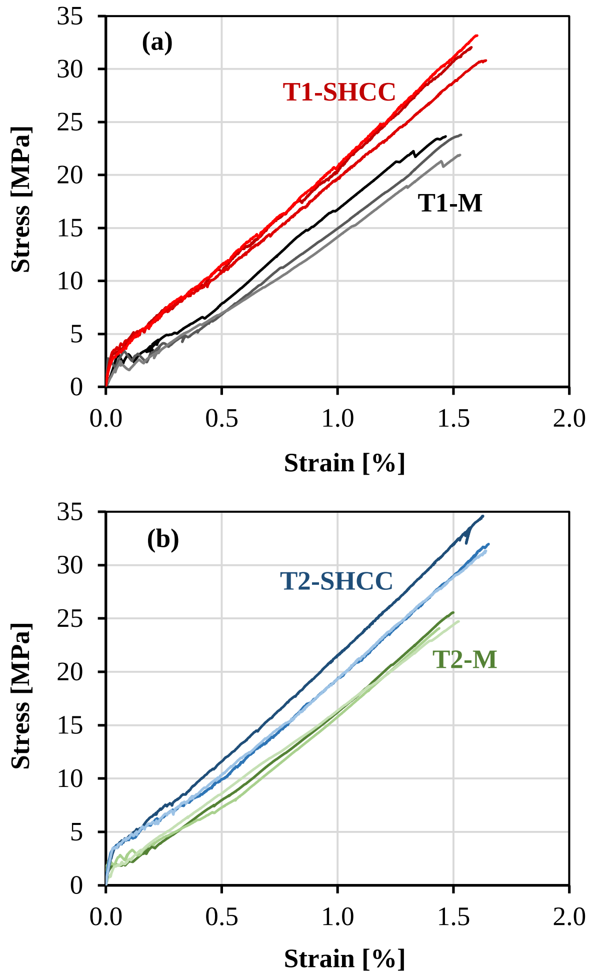


**Figure 7**: Uniaxial tensile behavior of the textile reinforced composites T1-M and T2-M and of the composites with hybrid fiber reinforcement T1-SHCC and T2-SHCC.

Note that the presented plain matrices were specifically developed for high-strength SHCC, meaning that their finely grained nature and notable brittleness were targeted properties. The typical matrices for TRC are coarser, less brittle and exhibit less spalling [3,12]. However, the exaggerated comparison at hand are aimed at indicating on the necessity of spatial micro-confinement of the matrix in case of severe mechanical or environmental actions.

The cracking behavior of the composites is demonstrated in Figure 10, based on DIC evaluations. As summarized in Table 5, the average crack widths of T1-M and T1-SHCC at the strain level of 0.2 % are 267 µm and 22 µm, respectively, with an average crack spacing of 150 mm within the 150 mm gauge length (only one crack) in the case of T1-M and 11 mm (14 cracks) in the case of T1-SHCC. The addition of short fibers reduces the crack width significantly disregarding the type of textile coating.

Besides the increased cracking stresses and improved crack control, the addition of short fibers leads to an increased tensile strength, i.e. failure stress of the textile yarns. For explaining this phenomenon, the effect of the short-fiber reinforcement on the bond properties and anchorage characteristics of the textile yarns must be investigated in detail.

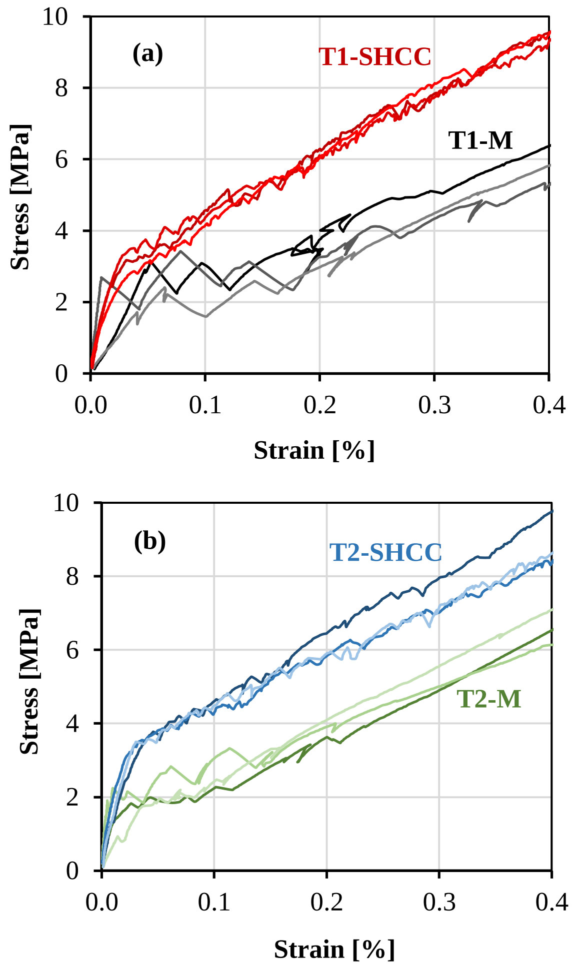


**Figure 8**: Cracking behavior of the investigated composites in the initial loading phase can be recognized from the unsteadiness of the stress-strain curves.

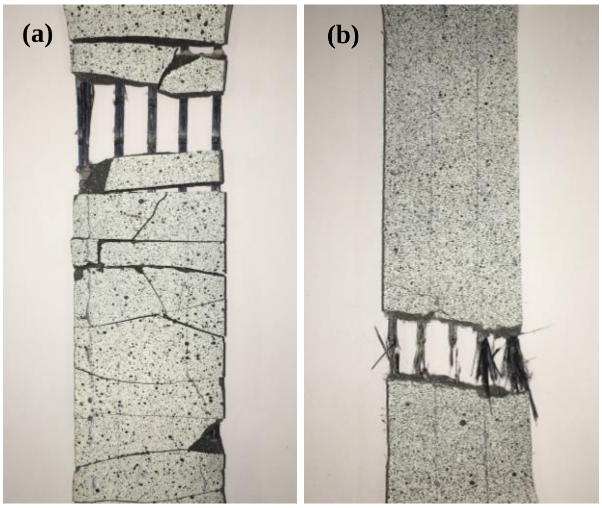


**Figure 9**: Damaged (a) T1-M and (b) T1-SHCC specimens after tension tests.

**Table 4**: Results of the uniaxial tension tests as average values, standard deviations are given in parentheses

| | T1-M | T1-SHCC | T2-M | T2-SHCC |
|---|---|---|---|---|
| Tensile strength (MPa) | 23.1 (1.1) | 32.0 (1.2) | 24.8 (0.7) | 32.6 (1.7) |
| First-crack stress (MPa) | 2.4 (0.6) | 3.0 (0.5) | 1.5 (0.5) | 3.4 (0.1) |
| Ultimate strain (%) | 1.5 (0.0) | 1.6 (0.0) | 1.5 (0.0) | 1.6 (0.0) |
| Work-to-fracture [kJ/m$^3$] | 176.8 (8.0) | 272.5 (5.8) | 183.8 (16.0) | 278.1 (12.9) |

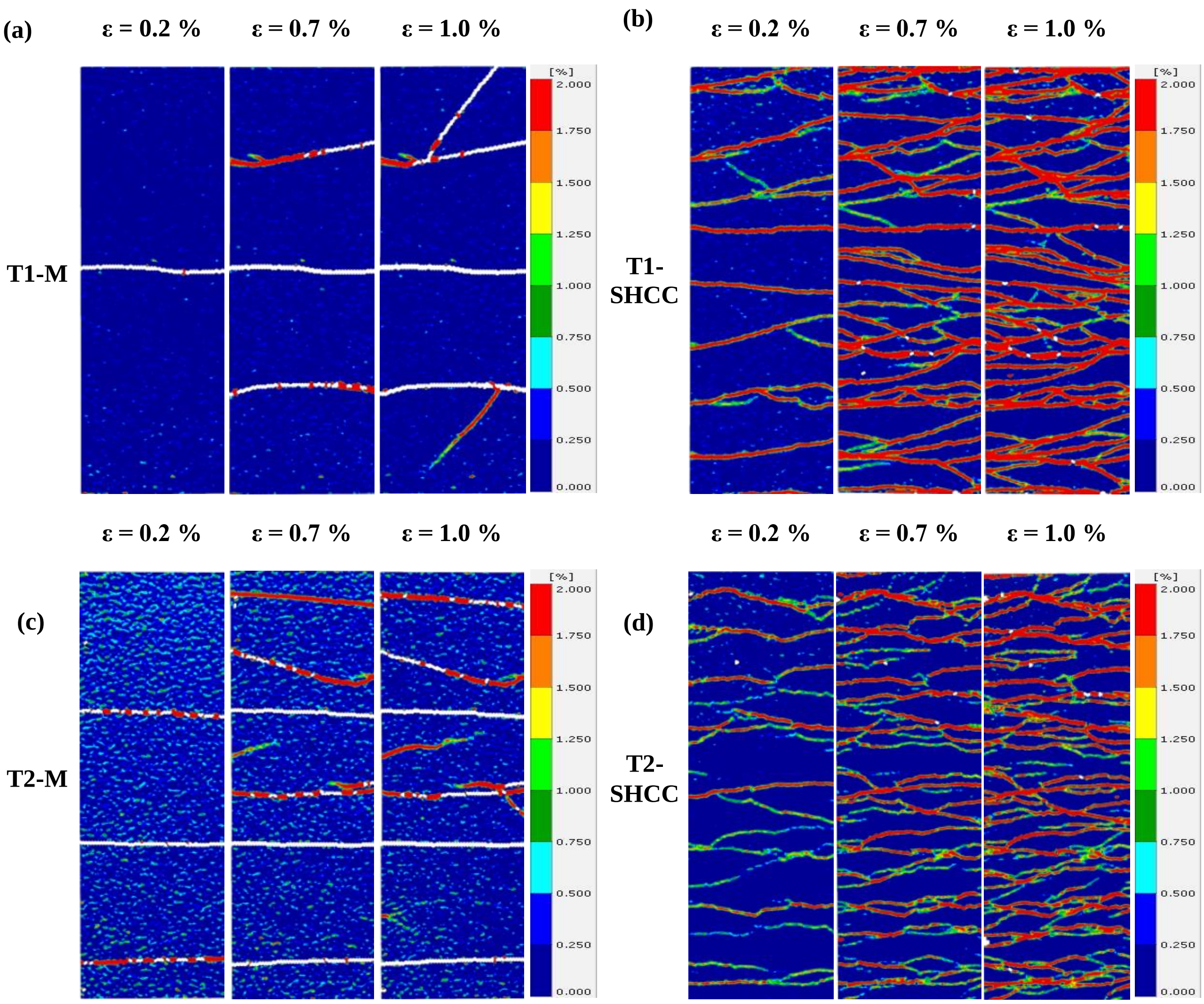


**Figure 10**: Representative crack patterns at the global strain levels of 0.2 %, 0.7 % and 1.0 % for (a) T1-M, (b) T1-SHCC, (c) T2-M and (d) T2-SHCC.

**Table 5**: Average width and crack number at the strain levels of 0.2 %, 0.7 % and 1.0 % for the representative specimens subjected to uniaxial tension tests

| | T1-M | T1-SHCC | T2-M | T2-SHCC |
|---|---|---|---|---|
| Average crack width at 0.2 % strain level $\omega_{crack\text{-}0.2\ \%}$ [µm] | 267 | 22 | 109 | 20 |
| Average crack spacing at 0.2 % strain level $S_{crack\text{-}0.2\ \%}$ [mm] | 150 | 11 | 50 | 9 |
| Average crack width at 0.7 % strain level $\omega_{crack\text{-}0.7\ \%}$ [µm] | 274 | 30 | 134 | 25 |
| Average crack spacing at 0.7 % strain level $S_{crack\text{-}0.7\ \%}$ [mm] | 38 | 5 | 19 | 4 |
| Average crack width at 1.0 % strain level $\omega_{crack\text{-}1.0\ \%}$ [µm] | 293 | 40 | 154 | 33 |
| Average crack spacing at 1.0 % strain level $S_{crack\text{-}1.0\ \%}$ [mm] | 30 | 4 | 17 | 3 |

The epoxy-sand coating had no significant effect on the cracking stress of the matrix and failure stress of the carbon yarns, but it had a measurable influence on the crack pattern and crack width. The extremely strong bond between the extra-coated yarns and the SHCC matrix yielded a lower crack spacing and crack width, compared to the standard acrylate coating, see Figure 10 and Table 5.

The better stress transfer from the yarns to the matrix allowed an enhanced local activation of the SHCC material, while the compatibility of these two materials in terms of strain capacity ensured that no early crack localization occurred in SHCC, as it would happen in the case of a longitudinal reinforcement with superior strain capacity

## 5 CONCLUSIONS

Hybrid fiber reinforced composites consisting of SHCC matrices and continuous textile reinforcement exhibit superior mechanical properties, crack control and damage tolerance in comparison to ordinary TRC.

The enhancement in the bond strength between carbon yarns and SHCC leads to a better activation of the quasi-ductility of SHCC, which ensures a higher degree of crack saturation and lower crack widths.

Different types of textile materials will be involved in future studies for a more detailed analysis of the effect of textile elongation capacity on the overall composite behavior.

Furthermore, the effect of high strain rates will be investigated in respect of the application of such hybrid fiber reinforced composites as strengthening layers for the enhancement of existing jeopardized concrete structures.

## ACKNOWLEDGMENTS

The authors express their great gratitude to the German Research Society (Deutsche Forschungsgemeinschaft - DFG) for the financial support provided within the framework of the Research Training Group GRK 2250. Credit is also given to Mr. Kai Uwe Mehlisch for his valuable contribution in performing the experiments.

## REFERENCES

[1] Li, V.C., 2003. On engineered cementitious composites (ECC). *Journal of advanced concrete technology*. **1(3)**:215-30.

[2] Mechtcherine, V., 2013. Novel cement-based composites for the strengthening and repair of concrete structures. *Construction and building materials*. **41**:365-73.

[3] Butler, M., Mechtcherine, V. and Hempel, S., 2009. Experimental investigations on the durability of fibre–matrix interfaces in textile-reinforced concrete. *Cement and Concrete Composites*. **31(4)**:221-31.

[4] Mechtcherine, V. and Curosu, I., 2017. Mineral-Bonded Composites for Enhanced Structural Impact Safety – A New Research Training Group GRK 2250 of the German Research Society. *In: Prodedia Engineering. 6th International Workshop on Performance, Protection & Strengthening of Structures under Extreme Loading, PROTECT2017*, December 11-12, 2017, Guangzhou, China; **210**:182-85.

[5] Gong, T., Heravi, A.A., Curosu, I. and Mechtcherine, V., 2018. Effect of textile reinforcement on the tensile behavior of strain-hardening cement-based composites (SHCC) under quasi-static and impact loading. *In: Proc. 5th International Conference on Protective Structures (ICPS5),* August 20-24, 2018, Poznan, Poland; pp.558-67.

[6] Curosu, I., Mechtcherine, V., Forni, D. and Cadoni, E., 2017. Performance of various strain-hardening cement-based composites (SHCC) subject to uniaxial impact tensile loading. *Cement and Concrete Research*. **102**:16-28.

[7] Curosu, I., Liebscher, M., Mechtcherine, V., Bellmann, C. and Michel, S., 2017. Tensile behavior of high-strength strain-hardening cement-based composites (HS-SHCC) made with high-performance polyethylene, aramid and PBO fibers. *Cement and Concrete Research*. **98**:71-81.

[8] Fact Sheet, Ultra High Molecular Weight Polyethylene Fiber Form Dyneema, Eurofibers, 2010. https://issuu.com/eurofibers/docs/name8f0d44.

[9] Soranakom, C. and Mobasher, B., 2010. Modeling of tension stiffening in reinforced cement composites: Part I. Theoretical modeling. *Materials and structures*. **43(9)**:1217-30.

[10] Colombo, I. G., Magri, A., Zani, G., Colombo, M. and Di Prisco, M., 2013. Erratum to: Textile Reinforced Concrete: experimental investigation on design parameters. *Materials and structures*. **46(11)**:1953-71.

[11] Yao, Y., Silva, F. A., Butler, M., Mechtcherine, V., and Mobasher, B., 2015. Tension stiffening in textile-reinforced concrete under high speed tensile loads. *Cement and Concrete Composites*. **64**:49-61.

[12] Barhum, R. and Mechtcherine, V., 2012. Effect of short, dispersed glass and carbon fibres on the behaviour of textile-reinforced concrete under tensile loading. *Engineering Fracture Mechanics*. **92:**56–71.